

Test-time Adaptation Meets Image Enhancement: Improving Accuracy via Uncertainty-aware Logit Switching

Shohei Enomoto*, Naoya Hasegawa[†], Kazuki Adachi*, Taku Sasaki*,
Shin'ya Yamaguchi*[‡], Satoshi Suzuki* and Takeharu Eda*

*NTT, Tokyo, Japan [†]University of Tokyo, Tokyo, Japan [‡]Kyoto University, Kyoto, Japan

{shohei.enomoto, kazuki.adachi, taku.sasaki, shinya.yamaguchi, satoшихv.suzuki, takeharu.eda}@ntt.com

[†]hasegawa-naoya410@g.ecc.u-tokyo.ac.jp

Abstract—Deep neural networks have achieved remarkable success in a variety of computer vision applications. However, there is a problem of degrading accuracy when the data distribution shifts between training and testing. As a solution of this problem, Test-time Adaptation (TTA) has been well studied because of its practicality. Although TTA methods increase accuracy under distribution shift by updating the model at test time, using high-uncertainty predictions is known to degrade accuracy. Since the input image is the root of the distribution shift, we incorporate a new perspective on enhancing the input image into TTA methods to reduce the prediction’s uncertainty. We hypothesize that enhancing the input image reduces prediction’s uncertainty and increase the accuracy of TTA methods. On the basis of our hypothesis, we propose a novel method: Test-time Enhancer and Classifier Adaptation (TECA). In TECA, the classification model is combined with the image enhancement model that transforms input images into recognition-friendly ones, and these models are updated by existing TTA methods. Furthermore, we found that the prediction from the enhanced image does not always have lower uncertainty than the prediction from the original image. Thus, we propose logit switching, which compares the uncertainty measure of these predictions and outputs the lower one. In our experiments, we evaluate TECA with various TTA methods and show that TECA reduces prediction’s uncertainty and increases accuracy of TTA methods despite having no hyperparameters and little parameter overhead.

Index Terms—Test-Time Adaptation, Image Enhancement, Uncertainty

I. INTRODUCTION

Deep neural networks (DNNs) have achieved remarkable success in various computer vision applications, such as classification, segmentation, and object detection. However, DNNs have a problem with accuracy degradation when the data distribution shifts between training and testing. This problem occurs frequently in outdoor environments, such as autonomous driving and smart cities, due to changes in weather and brightness [1]–[3]. To solve this problem, DNNs need to be more robust to these distribution shifts.

One of the most practical settings to improve the robustness of DNNs is Test-time Adaptation (TTA). In the TTA setting, a pre-trained model is given, and the model is tested and updated simultaneously using unlabeled target data. The model

maintains accuracy by adapting to distribution shifts during testing. The TTA setting has the advantages such as working under realistic distribution shifts [4]–[6] and privacy protection because it does not store data. This setting has attracted the attention of many researchers because of its generality, flexibility, and practicality.

The typical TTA method uses predictions to update a model [7]. Under continuously changing target distributions, the prediction becomes highly uncertain and noisy, leading to accuracy degradation [8]. To address this degradation, existing studies have proposed uncertainty reduction through an improved TTA framework [4] and an improved loss function without uncertain predictions [8]. Although these methods have increased accuracy by eliminating the adverse effects of uncertain predictions, a large gap remains between the accuracy of the source and target distributions. This is because these methods use original input images, which are the root of the distribution shift, without any improvements. Therefore, we focus on improving image quality, while existing TTA studies have focused on improving the framework and loss. We hypothesize that improving image quality can reduce the uncertainty of the predictions and that updating the model by using such images further increases the accuracy of TTA methods.

To generate high-quality images, we use an image enhancement model [9]–[16], which transforms distorted images into ones that can be easily recognized by classification models. Since enhanced images are known to increase the accuracy of classification models, we hypothesize that they decrease the uncertainty of the predictions and are suitable for TTA methods. On the basis of our hypothesis, we propose a novel method, Test-time Enhancer and Classifier Adaptation (TECA), which combines an image enhancement model and a classification model into a single one and updates it in the TTA manner. By updating the unified model during testing, TECA provides predictions with low-uncertainty even under unknown shifted distributions, allowing stable updating of TTA methods. In addition to combining two models, we present an important finding that the image enhancement

model does not always reduce the prediction’s uncertainty, indicating that updating classification models with enhanced images is not always appropriate. To overcome this problem, we propose *Logit Switching* (LS). LS compares the uncertainty of predictions from the original image and enhanced one, and outputs the one with the lower uncertainty. Furthermore, we introduce two modules: *Synchronizing Parameter Updating Speed* (SPUS), which balances the different speeds of the model update in LS and stabilizes the update, and *Freezing Batch Normalization Statistics* (FBNS), which preserves the source knowledge of an image enhancement model necessary to enhance the image quality. By incorporating LS with SPUS and FBNS, TECA can effectively reduce the uncertainty of the classification predictions, and as a result, the TTA methods increase the accuracy much more. TECA focuses on transforming the input images, which existing TTA methods do not deal with, and can be easily combined with existing TTA methods.

We conducted experiments with the continual TTA task [4] on the ImageNet dataset [2] and with the domain generalization benchmarks [17]. We show that combining state-of-the-art TTA methods with TECA reduces prediction’s uncertainty and increases accuracy. TECA shows higher training efficiency than simply increasing the number of the classification model parameters, despite its low parameter overhead. We also show that TECA works well with a variety of classification model architectures.

The contributions of this paper are as follows:

- We propose a novel method, TECA, which updates the image enhancement and classification models at test time from predictions with low uncertainty. TECA is simple yet effective, with no hyperparameters and low overhead, but improves the accuracy of the TTA methods.
- We show in experiments that TECA decreases the error rate of TTA methods for various distribution shifts. TECA is more parameter effective than simply increasing the number of the classification model parameters and works with a variety of classification models.

II. RELATED WORK

A. Test-time Adaptation

Test-time Adaptation (TTA) is a setting that updates the model under distribution shift online with each mini-batch, without accessing the source dataset or labeled target data. This problem setting has attracted much attention because it is more practical and has fewer constraints than Domain Generalization and Domain Adaptation. As pioneering work, Wang *et al.* [7] proposed TTA setting. They found that the entropy of predictions correlates with accuracy and proposed Tent, which updates a classification model through entropy minimization. To further improve the performance of TTA methods, numerous studies were conducted, such as using data augmentation to make predictions consistent [18]–[20], introducing a teacher-student training framework [4], [21], using meta-learning [22], [23], and aligning intermediate

representations with prototypes [24]–[28]. Since models are continuously updated online in the TTA setting, reducing their computational cost [8], [29] and avoiding catastrophic forgetting [4], [8], [21] are also important research problems. In addition, the application of TTA to various recognition tasks [30]–[37] and its extension to more realistic distribution shift problem settings [4]–[6] has also attracted attention.

Although many TTA studies have been conducted, a large gap remains between the accuracy of the source and target distributions. To close this gap, we incorporate a new perspective on enhancing the input image into TTA methods. We use an image enhancement model to transform the input image into a recognition-friendly image, thus increasing the performance of TTA methods.

B. Input Adaptation

Input adaptation improves recognition accuracy by transforming input images into ones that are easier to recognize, *i.e.*, *recognition-friendly*, images. Here we introduce two approaches: image enhancement, an image transformation method based on DNNs; and visual prompt adaptation, which adds trainable noise to the input image.

1) *Image Enhancement*: In image enhancement, the DNN, which we call the image enhancement model, learns image transformations that minimize losses of the recognition model. Sharma *et al.* [38] improves recognition accuracy by emphasizing image-specific details with a DNN-based enhancement filter. The subsequent work [9]–[16] uses DNN to transform corrupted images into recognition-friendly ones.

We aim to incorporate these input adaptation methods into TTA methods to further increase accuracy by reducing prediction’s uncertainty from enhanced images. Updating an image enhancement model at test time has never been conducted and allows for predictions with low-uncertainty even under distribution shift. Furthermore, to avoid harmful updates caused by high-uncertainty prediction, we propose switching to the predictions with low-uncertainty ones to update the model.

2) *Visual Prompt Adaptation*: To improve the robustness of DNNs, several studies have been conducted to update the visual prompt [39], [40], which is trainable noise, at test time [41]–[43]. Unlike the image enhancement model, the visual prompt does not use a DNN, but transforms the input image by adding the noise. In the visual prompt adaptation, the recognition model is frozen and only the visual prompt is updated during testing, as well as in TTA methods.

Our study is similar to these studies in terms of combining the image enhancer and TTA methods, although it differs in that it simultaneously updates the image enhancement model and the classification model from the switched low-uncertainty predictions.

TABLE I

MAIN DIFFERENCES BETWEEN THE TECA PROBLEM SETTING AND THE EXISTING ADAPTATION PROBLEM SETTING. EXISTING SETTINGS MAINTAIN CLASSIFICATION ACCURACY UNDER DISTRIBUTION SHIFT BY UPDATING CLASSIFICATION MODELS OR TRANSFORMING TARGET IMAGES AT THE TEST TIME. THE TECA SETTING UPDATES PARAMETERS IN BOTH THE CLASSIFICATION AND THE IMAGE ENHANCEMENT MODELS AT THE TEST TIME. v_{ψ_0} IS A PRETRAINED VISUAL PROMPT.

Setting	Updated	Given
TTA	θ_t	$f_{\theta_0}^{\text{cls}}$
Image Enhancement	–	$f_{\theta_0}^{\text{cls}}, f_{\phi_0}^{\text{enh}}$
Visual prompt adaptation	v_{ψ_t}	$f_{\theta_0}^{\text{cls}}, v_{\psi_0}$
TECA	θ_t, ϕ_t	$f_{\theta_0}^{\text{cls}}, f_{\phi_0}^{\text{enh}}$

III. TEST-TIME ENHANCER AND CLASSIFIER ADAPTATION (TECA)

A. Problem Definition

Given the classification model $f_{\theta_0}^{\text{cls}}(x)$ and the image enhancement model $f_{\phi_0}^{\text{enh}}(x)$ trained on the source dataset, our goal is to update these models simultaneously during testing and adapt them to the target domain to increase their accuracy. We treat these two models as one model f_{Θ_0} , where $\Theta_0 = [\theta_0, \phi_0]$, and apply TTA methods. Provided with the mini-batch of target data x_t^T at time t sampled from the unlabeled target domain dataset, x_t^T is fed into the model f_{Θ_t} and the model outputs a prediction $f_{\Theta_t}(x_t^T)$. The model is then updated $\Theta_t \rightarrow \Theta_{t+1}$ from $f_{\Theta_t}(x_t^T)$. The loss used to update the model depends on the TTA method applied (*e.g.*, Tent uses entropy minimization).

Table I lists the main differences between the TECA setting and the existing adaptation settings. Neither setting requires access to the source dataset and target data labels, although each setting has different updated parameters and given components. In the TTA setting, the classification model is updated at test time by using unlabeled target data. The image enhancement and visual prompt adaptation settings transform the target image during testing but the given components are different. In the image enhancement setting, an image enhancement model transforms the target image into a recognition-friendly one. In the visual prompt adaptation setting, the visual prompt, the trainable noise that increases recognition accuracy, is updated during testing. The TECA problem setting updates both the classification and image enhancement models at test time.

B. Analysis of Image Quality, Uncertainty, and Error Rate

In this paper, we hypothesize that improving image quality can reduce the uncertainty of the predictions and that updating the model by using such images further increases the accuracy of TTA methods. To verify our hypothesis, we analyzed the relationship between error rate and uncertainty in various image quality, as shown in Fig. 1. We found that the error rate and entropy were inversely proportional to the image quality. In other words, the higher the image quality, the smaller the error rate and entropy, and the lower the image quality, the

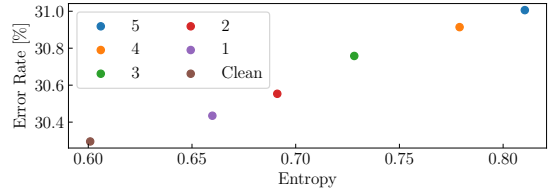


Fig. 1. Preliminary experiments on our hypothesis. We updated ResNeXt [44] with Tent on the CIFAR-100-C dataset and measured error rates and entropy. We tested clean images and ones corrupted at five severity levels, where higher severity indicates stronger corruption and lower image quality, while lower severity indicates cleaner images and higher image quality.

Algorithm 1 Test-Time Enhancer and Classifier Adaptation (TECA)

Initialization: Model f_{Θ_0} composed of source pre-trained classification model $f_{\theta_0}^{\text{cls}}$ and image enhancement model $f_{\phi_0}^{\text{enh}}$.

Input: For each time step t , current stream of data x_t .

- 1: Get the enhanced image $f_{\phi_t}^{\text{enh}}(x_t)$.
- 2: Calculate predictions $f_{\theta_t}^{\text{cls}}(x_t)$ and $f_{\theta_t}^{\text{cls}}(f_{\phi_t}^{\text{enh}}(x_t))$.
- 3: Compare the confidence score of predictions and select the higher one as $f_{\Theta_t}(x_t)$ by Equation (1).
- 4: Calculate gradients ∇_{Θ} by TTA loss.
- 5: Rescale gradients ∇_{ϕ} by Equation (2).
- 6: Update Θ_t using gradient descent.

Output: Prediction $f_{\Theta_t}(x_t)$; Updated model $f_{\Theta_{t+1}}$.

larger the error rate and entropy. This suggests that high-quality images improve the accuracy of the TTA method, which supports our hypothesis.

C. Methodology

Fig. 2 and Algorithm 1 show the overview and pseudo-code of TECA. To further reduce prediction’s uncertainty and increase the accuracy of existing TTA methods, we study improvements in image quality. Fig. 3 shows the original and enhanced images and their confidence score. We found that performing classification with enhanced images does not always achieve a higher confidence score, an uncertainty measure, than one with the original images. The straightforward input adaptation approach uses only enhanced images, and thus it is not suitable in the TTA setting. Therefore, we propose LS that compares the uncertainty of the predictions from the original and enhanced images and then outputs the lower one. Furthermore, we introduce two modules to increase the stability of TECA: SPUS to align the parameter update speeds of the classification and image enhancement models, and FBNS to freeze the BN statistics of the image enhancement model to retain source knowledge for recognition-friendly image transformation.

Given an image enhancement model, TECA can be easily combined with existing TTA methods to further increase accuracy, since TECA has no hyperparameters. We describe the details of our methodology in the following paragraphs.

a) *Given Models.*: In the TECA setting, we assume that a classification model and an image enhancement model

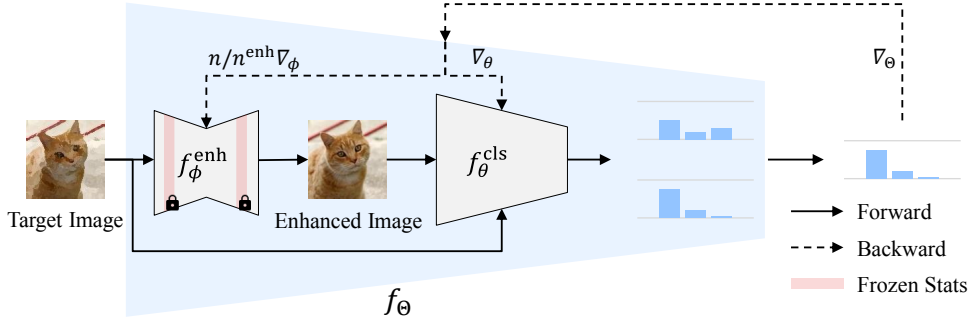


Fig. 2. Overview of TECA. The image enhancement model transforms the target image into a recognition-friendly one. The classification model predicts both original and recognition-friendly images. TECA compares the uncertainty of the predictions and switches predictions to the lower one. The model is updated from the prediction using the TTA methods. At this time, the gradient of the image enhancement model is rescaled to align the parameter update speed of each model that stabilizes the updates. Additionally, the BN statistics of the image enhancement model are frozen to preserve source knowledge.

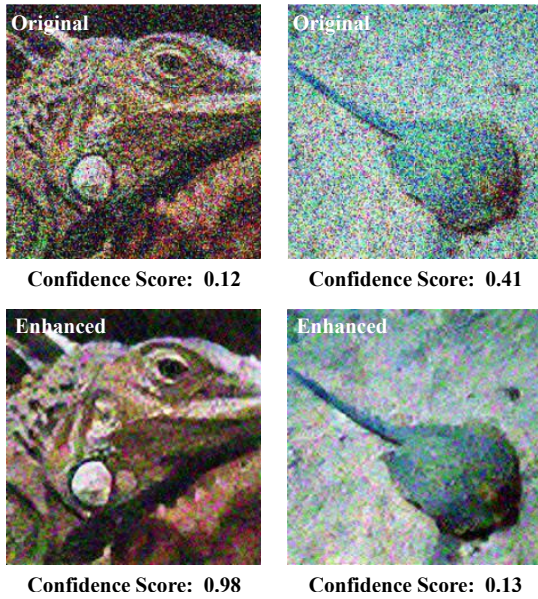


Fig. 3. Gaussian noise at severity level 5 images and URIE [9]-enhanced images and their confidence score in the ImageNet-C dataset. The top and bottom rows are the original and enhanced images, respectively.

that are pre-trained on the source dataset are given as stated in Section III-A. The classification model does not require a special process for the TECA setting. In this paper, we use URIE [9] as an image enhancement model. URIE has a U-Net [45] type DNN structure that improves the robustness of the classification model with a few trainable parameters. URIE is trained to minimize the loss of the frozen pre-trained classification model on the source dataset with artificial distribution shifts (*e.g.*, data augmentation). We refer to this frozen pre-trained classification model as *enhancer partner*.

b) Logit Switching (LS).: As shown in Fig. 3, the image enhancement model does not always reduce prediction’s uncertainty. Adapting models from uncertain predictions should be avoided because it leads to error accumulation and catastrophic forgetting [8]. Therefore, to solve this problem, we propose LS that obtains predictions from both the enhanced and original images, compares the predictions with confidence scores, and

then switches the prediction to the higher confidence one and uses it for model updating. The LS is shown in Equation (1).

$$f_{\Theta_t}(x) = \begin{cases} f_{\theta_t}^{cls}(f_{\phi_t}^{enh}(x)) & (\text{if } \max(p^{enh}) > \max(p^{cls})) \\ f_{\theta_t}^{cls}(x) & (\text{else}), \end{cases} \quad (1)$$

where x is an input image and p^{enh} and p^{cls} are the softmax probability predictions from the enhanced and original images, respectively.

c) Synchronizing Parameter Updating Speed (SPUS).: Whereas the classification model f_{θ}^{cls} is updated from all predictions, the image enhancement model f_{ϕ}^{enh} is not updated if the predictions from the original images are selected because there is no backward path. This causes a difference in the updated speed, which harms the accuracy [46]. To prevent this, inspired by [46], we introduce SPUS, which rescales the gradient and ensures a similar parameter updating speed. Let n be the batch size at the test time, n^{enh} is the number of enhanced images employed in Equation (1), and we rescale the gradient of the image enhancement model by

$$\nabla_{\phi} \leftarrow (n/n^{enh})\nabla_{\phi}. \quad (2)$$

d) Freezing BN Statistics (FBNS).: *BN Adapt* [47] only updates the BN statistics from input data at the test time. Since it is a simple and effective TTA method, many TTA methods have built-in BN Adapt. However, we experimentally found that BN Adapt is not suitable for the image enhancement model and decreases the accuracy (see Section IV-C1 for details). We solve this problem by freezing the BN statistics of the image enhancement model during testing.

IV. EXPERIMENTS

We combined TECA with the several TTA methods and evaluated them in the standard continual TTA (CTTA) [4] task and domain generalization benchmarks. We show that TECA increases accuracy of existing TTA methods despite the small overhead and works with a variety of classification models.

A. Experimental Setup

a) *Dataset and Tasks.*: For the standard CTTA task, we conducted experiments on the ImageNet-C dataset [2] to evaluate the robustness against common image corruption. This dataset contains 15 types of corruptions with 5 levels of severity. Following existing studies, we used the largest corruption severity level 5 and 5,000 samples were extracted from the test set by RobustBench to evaluate the error rate in each corruption. For the domain generalization benchmarks, we experimented with four datasets, VLCS, PACS, Office-Home, and TerraIncognita, using the DomainBed library [17].

We experimented with a classification model pre-trained on the ImageNet1K dataset published by torchvision (excluding DeiT [48]), with TTA methods. We evaluated the avoidance of error accumulation and catastrophic forgetting by TTA methods in the CTTA task, where the distribution is continuously changing. For the standard CTTA task, we evaluated TTA methods on a corrupted test set and then evaluate it on the next corrupted test set without resetting the model and optimizer.

b) *TTA Methods.*: We refer to the method that uses only the classification model as *Source* and the method that uses the enhanced image by URIE as input to the classification model as *Input Adapt*. In these methods, the models are frozen and not adapted at test time. For the CTTA task, we used four TTA methods. BN Adapt [47] updates only BN statistics at the test time. Note that when we combine TECA with BN Adapt, we do not freeze BN statistics. *Tent* [7] updates only the BN layer through entropy minimization. *EATA* [8] extends Tent by efficient training with active sample selection and avoiding catastrophic forgetting with Elastic Weight Consolidation. *CoTTA* [4] uses a self-training framework, augmentation-averaged pseudo-labels, and stochastic restoration to deal with error accumulation and catastrophic forgetting in continually changing distributions. For the domain generalization benchmarks, we used *T3A* [28], a TTA method which adjusts the linear classifier (the last layer of DNNs) at test-time.

c) *Implementation Details.*: For the CTTA task, we used SGD with momentum 0.9, batch size 64, learning rate of 0.01 for CoTTA and RoTTA, and 0.00025 for Tent and EATA. For the domain generalization benchmarks, we used batch size 32. The other hyperparameters for each method and task follow the original setting.

The original training setup for URIE uses the corruption dataset and is not suitable for the experimental setup for the CTTA task, which is evaluated on the corruption dataset. Therefore, we trained URIE on the augmented dataset in accordance with the blind setting proposed in [15]. For the CTTA task, we used AugMix [49] and DeepAugment [50]. As with the AugMix paper, data augmentations used by AugMix¹ do not include the test corruption in the ImageNet-C dataset. For the domain generalization benchmarks, we used AugMix with four additional operations² because there are no data

¹autocontrast, equalize, posterize, rotate, solarize, shear x, shear y, translate x, translate y

²color, contrast, brightness, sharpness

augmentations that overlap with the test set. In this setting, URIE learns to enhance the features needed to classify out-of-distribution data from diverse data generated by the data augmentation. This enables URIE to increase classification accuracy for unknown distribution shifts, even though it does not learn the distribution shifts at test time. We used ResNet-50 as the enhancer partner when training URIE, except for the experiments in Section IV-B4.

B. Experimental Results

1) *Results of the CTTA Task*: Table II shows the results of the standard CTTA task. Combining TTA methods with TECA reduces error rates for almost all corruptions except for a few and on average improves error rates for all methods. The combination of Tent and TECA outperforms the state-of-the-art TTA methods, EATA and CoTTA, indicating that adaptation efficiency with TECA is high. This result indicates that enhancing the input image, which is the root of the distribution shift, is more beneficial for TTA methods than improving the framework or loss. The combination of CoTTA and TECA shows the best overall result, reducing the average error rate by 3.89 points compared with CoTTA alone.

2) *Results of the Domain Generalization Benchmarks*: Table III shows the results of the domain generalization benchmarks. TECA improves the accuracy of T3A and shows the best results. This result indicates the effectiveness of TECA for various types of distribution shifts.

3) *Trade-off between Error Rate and Number of Parameters*: TECA uses an image enhancement model, which increases the number of trainable parameters. In general, the error rate decreases as the number of trainable parameters increases. To evaluate the parameter efficiency, we compared the TTA methods and its combination with TECA on ResNet with different numbers of parameters. The results are shown in Fig. 4. TECA improves the trade-offs of all TTA methods despite the number of parameters for URIE, the image enhancement model used in this study, being 0.67×10^6 , which is sufficiently small compared with ResNet (e.g., ResNet-50 has 25.56×10^6 parameters). The results show that using TECA is more parameter-efficient than simply increasing the number of classification model parameters.

4) *Other Architectures*: The image enhancement model is more effective when used in conjunction with the enhancer partner because the image enhancement model is trained to minimize the loss of the enhancer partner [15]. We conducted experiments to investigate whether TECA improves the TTA methods when using a different enhancer partner than the one used when training the image enhancement model. The results are shown in Table IV. Note that DeiT has the same architecture as ViT [51] and does not have a BN layer; instead we update the layer normalization layer [25]. For layer normalization layers, BN-adapt cannot be used, and TECA only works as LS. The image enhancement model trained with ResNet-50 shows a lower error rate for similar architectures, ResNeXt-50 and Wide ResNet-50, while the error rate increases for a completely different architecture,

TABLE II

CLASSIFICATION ERROR RATE OF RESNET-50 FOR THE STANDARD IMAGENET CTTA TASK. MEAN INDICATES THE AVERAGE ERROR RATE FOR ALL CORRUPTION TEST SETS. THE BEST AND SECOND RESULTS ARE **BOLDED** AND UNDERLINED.

Time	$t \rightarrow$																
Method	TECA	Gaussian	shot	impulse	defocus	glass	motion	zoom	snow	frost	fog	brightness	contrast	elastic_trans	pixelate	jpeg	Mean ↓
Source		95.30	94.58	95.30	84.86	91.08	86.84	77.18	84.38	79.70	77.26	44.42	95.58	85.24	76.92	66.68	82.35
Input Adapt		83.10	82.62	83.04	84.12	90.32	85.08	77.82	80.34	74.72	70.90	44.88	89.34	81.06	62.18	59.48	76.60
BN Adapt		87.62	87.46	87.78	87.80	87.98	78.28	64.42	67.64	70.62	54.84	36.44	89.24	58.04	56.42	66.54	72.07
BN Adapt	✓	83.24	82.42	83.48	86.66	86.10	75.70	64.28	66.34	68.00	54.92	35.98	82.90	57.36	54.26	62.42	69.60
Tent		85.64	79.98	78.14	82.20	<u>79.22</u>	71.04	59.12	65.58	66.38	55.52	40.52	80.46	55.58	53.44	59.14	67.46
Tent	✓	79.08	<u>73.54</u>	72.92	80.74	78.86	<u>69.52</u>	59.54	65.02	64.76	55.06	40.50	77.56	56.02	53.40	58.04	65.64
EATA		84.04	80.16	80.96	83.52	82.58	70.64	<u>58.40</u>	62.00	65.72	49.80	34.98	82.20	53.38	49.94	59.98	66.55
EATA	✓	77.44	73.26	<u>74.90</u>	<u>81.36</u>	81.02	68.96	58.18	61.06	<u>63.58</u>	48.74	<u>35.06</u>	77.74	52.58	48.82	56.42	<u>63.94</u>
CoTTA		87.34	86.18	84.36	85.82	84.34	75.06	63.44	63.28	63.92	52.32	38.54	<u>73.14</u>	<u>51.06</u>	45.14	50.38	66.95
CoTTA	✓	81.04	77.68	76.74	82.24	79.64	69.56	59.74	<u>61.44</u>	61.06	<u>49.62</u>	38.66	66.16	49.70	44.22	48.40	63.06

TABLE III

CLASSIFICATION ACCURACY OF RESNET-50 FOR THE DOMAIN GENERALIZATION BENCHMARKS. WE EXPERIMENTED THREE TIMES AND REPORT THE MEAN AND STANDARD ERROR.

Method	TECA	VLCS	PACS	OfficeHome	TerraIncognita	Mean ↑
Source		76.4 ± 0.3	84.5 ± 0.8	66.8 ± 0.1	<u>45.5</u> ± 0.4	68.3
Input Adapt		75.8 ± 0.3	85.2 ± 0.7	66.8 ± 0.1	45.7 ± 1.0	68.4
T3A		76.8 ± 0.3	85.4 ± 0.6	<u>67.8</u> ± 0.2	43.5 ± 0.4	<u>68.4</u>
T3A	✓	<u>76.6</u> ± 0.3	86.1 ± 0.6	67.9 ± 0.2	44.6 ± 0.7	68.8

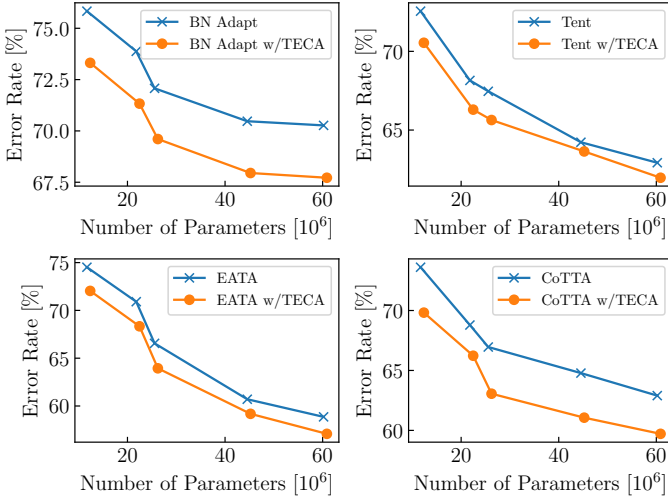


Fig. 4. Trade-off between error rate and number of parameters for the standard CTTA task. We compared the TTA method with TECA using ResNet-18, 34, 50, 101, and 152 as classification models. The blue and orange lines show TTA method without and with TECA.

DeiT-base. On the other hand, the image enhancement model trained with DeiT-base slightly reduces the error rate for all architectures. The updating of DeiT-small and DeiT-base by EATA shows catastrophic forgetting, while TECA prevents catastrophic forgetting of DeiT-small. In most experiments, TECA reduces the error rate of the TTA methods. The decrease in error rate for TECA is proportional to the decrease in error rate for Input Adapt. Even when Input Adapt increases the error rate, TECA decreases the error rate of all TTA methods

except Tent. This result indicates that the image enhancement model used by TECA may be trained with any classification model and has fewer limitations for TECA.

C. More Discussion

In this section, we conducted more detailed experiments on the standard CTTA task.

1) *Range for Updating Parameters:* Although TECA updates both the classification and image enhancement models, we evaluated the error rate when only the respective models are updated. The results are shown in Table V. We found that updating only the image enhancement model with BN Adapt results in an increased error rate. Since the image enhancement model improves classification accuracy by transforming corrupted images into ones that are closer to the source domain used for training, the results suggest that source domain knowledge, especially BN statistics, is highly important. For all other TTA methods except EATA, the error rate is increased by updating only the image enhancement model despite freezing the BN statistics. This result indicates that updating the image enhancement model from uncertain predictions with high entropy has a significantly negative impact. Updating only the classification model with TECA reduces the error rate for all TTA methods. Updating both models has the best results, even though updating only the image enhancement model increased the error rate. The average entropy when updating only the image enhancement model for Input Adapt, BN Adapt, Tent, EATA, and CoTTA was 3.31, 3.03, 2.88, 3.03, and 3.03, respectively. Although updating only the image enhancement model with TECA decreases accuracy, it also reduces average

TABLE IV
AVERAGE CLASSIFICATION ERROR RATE FOR DIFFERENT CLASSIFICATION AND IMAGE ENHANCEMENT MODELS FOR THE STANDARD CTTA TASK.

Classifier	TECA (Enhancer Partner)	Source	Input Adapt	BN Adapt	Tent	EATA	CoTTA
ResNeXt-50		79.34	N/A	70.81	63.80	62.72	63.69
	✓ (ResNet-50)	N/A	74.58	68.67	63.00	60.88	60.43
	✓ (DeiT-base)	N/A	78.69	69.61	63.58	61.23	61.71
WideResNet-50		79.41	N/A	70.22	62.97	62.54	63.61
	✓ (ResNet-50)	N/A	74.43	68.15	61.88	60.42	59.94
	✓ (DeiT-base)	N/A	79.31	69.05	62.51	60.94	60.86
DeiT-tiny		75.30	N/A	N/A	73.50	72.31	89.22
	✓ (ResNet-50)	N/A	72.96	72.36	70.15	68.77	70.18
	✓ (DeiT-base)	N/A	72.93	72.78	71.04	<u>69.17</u>	77.36
DeiT-small		62.43	N/A	N/A	58.65	99.08	55.95
	✓ (ResNet-50)	N/A	61.38	60.32	64.63	96.90	<u>54.54</u>
	✓ (DeiT-base)	N/A	60.05	59.80	57.47	54.66	53.49
DeiT-base		55.04	N/A	N/A	51.25	99.72	50.89
	✓ (ResNet-50)	N/A	56.98	54.30	52.16	99.65	<u>49.81</u>
	✓ (DeiT-base)	N/A	54.15	52.95	50.58	99.71	49.48

TABLE V
AVERAGE CLASSIFICATION ERROR RATE OF RESNET-50 WHEN CHANGING THE PARAMETER TO BE UPDATED. THE NUMBERS IN PARENTHESES INDICATE THE DIFFERENCE FROM WHEN THE MODEL IS NOT UPDATED.

Update	BN Adapt	Tent	EATA	CoTTA
Enhancer ϕ	77.85(1.25)	77.60(1.00)	76.56(-0.04)	77.41(0.81)
Classifier θ	69.66(-6.94)	65.85(-10.75)	64.13(-12.47)	63.52(-13.08)
Both Θ	69.60(-7.00)	65.64(-10.96)	63.94(-12.66)	63.06(-13.54)

entropy. Updating the model with high-entropy predictions causes error accumulation [8], while our method improves the stability of TTA methods by lowering the entropy of the predictions.

2) *Ablation Studies:* We evaluated the effectiveness of each of the three modules that further increase accuracy beyond simply combining and updating the classification and image enhancement models. The results are shown in Table VI. The improvement in error rate due to LS is significant, and in EATA, in particular, the model collapsed without LS. SPUS shows a slight improvement for Tent and EATA, while CoTTA decreases the error rate. Unlike other TTA methods, CoTTA uses all model parameters for training, so the impact of parameter update speed is significant. As described in Section IV-C1, BN Adapt is not suitable for training the image enhancement model, and removing BN Adapt from the TTA method reduces the error rate.

V. CONCLUSION

In this paper, we propose a new problem setting that combines and updates the classification model and the image enhancement model during testing, and a novel method, TECA, that further increases accuracy of existing TTA methods by updating both models from low-uncertainty predictions. To further increase the accuracy of TECA, we introduce two modules: SPUS and FBNS. Although TECA does not have hyperparameters and the overhead of trainable parameters is very small, its training efficiency is higher than simply

TABLE VI
AVERAGE CLASSIFICATION ERROR RATE OF RESNET-50 WHEN EACH OF THE THREE MODULES IS EXCLUDED. THE NUMBERS IN PARENTHESES INDICATE THE DIFFERENCES FROM THE TECA WITH ALL MODULES INCLUDED. BN ADAPT REQUIRES UPDATING THE BN STATISTICS AND DOES NOT UPDATE THE TRAINABLE PARAMETERS, SO SPUS AND FBNS ARE NOT EXCLUDED.

Excluded	BN Adapt	Tent	EATA	CoTTA
LS	71.39(1.79)	66.14(0.50)	99.52(35.58)	63.94(0.88)
SPUS	N/A	65.68(0.04)	63.95(0.00)	63.67(0.61)
FBNS	N/A	66.22(0.58)	64.17(0.23)	63.87(0.81)

increasing the number of the classification model parameters. We evaluated TECA in the continual TTA task and the domain generalization benchmarks. We find that TECA further increases the accuracy of state-of-the-art TTA methods in all experimental settings. Furthermore, more detailed experiments show the parameter efficiency and validity of TECA and that it works with a variety of classification models.

REFERENCES

- [1] S. Diamond, V. Sitzmann, F. Julca-Aguilar, S. Boyd, G. Wetzstein, and F. Heide, "Dirty pixels: Towards end-to-end image processing and perception," *ACM Transactions on Graphics (TOG)*, 2021.
- [2] D. Hendrycks and T. Dietterich, "Benchmarking neural network robustness to common corruptions and perturbations," in *International Conference on Learning Representations (ICLR)*, 2019.
- [3] O. Zendel, K. Honauer, M. Murschitz, D. Steiner, and G. F. Dominguez, "Wilddash - creating hazard-aware benchmarks," in *European Conference on Computer Vision (ECCV)*, 2018.
- [4] Q. Wang, O. Fink, L. Van Gool, and D. Dai, "Continual test-time domain adaptation," in *IEEE/CVF Conference on Computer Vision and Pattern Recognition (CVPR)*, 2022.
- [5] L. Yuan, B. Xie, and S. Li, "Robust test-time adaptation in dynamic scenarios," in *IEEE/CVF Conference on Computer Vision and Pattern Recognition (CVPR)*, 2023.
- [6] L. Jiang and T. Lin, "Test-time robust personalization for federated learning," in *International Conference on Learning Representations (ICLR)*, 2023.
- [7] D. Wang, E. Shelhamer, S. Liu, B. Olshausen, and T. Darrell, "Tent: Fully test-time adaptation by entropy minimization," in *International Conference on Learning Representations (ICLR)*, 2021.

- [8] S. Niu, J. Wu, Y. Zhang, Y. Chen, S. Zheng, P. Zhao, and M. Tan, "Efficient test-time model adaptation without forgetting," in *International Conference on Machine Learning (ICML)*, 2022.
- [9] T. Son, J. Kang, N. Kim, S. Cho, and S. Kwak, "Urie: Universal image enhancement for visual recognition in the wild," in *European Conference on Computer Vision (ECCV)*, 2020.
- [10] Y. Lee, J. Jeon, Y. Ko, B. Jeon, and M. Jeon, "Task-driven deep image enhancement network for autonomous driving in bad weather," in *IEEE International Conference on Robotics and Automation (ICRA)*, 2021.
- [11] D. Liu, B. Wen, X. Liu, Z. Wang, and T. S. Huang, "When image denoising meets high-level vision tasks: A deep learning approach," in *International Joint Conference on Artificial Intelligence (IJCAI)*, 2018.
- [12] Y. Pei, Y. Huang, Q. Zou, X. Zhang, and S. Wang, "Effects of image degradation and degradation removal to cnn-based image classification," *IEEE Transactions on Pattern Analysis and Machine Intelligence (TPAMI)*, 2021.
- [13] I. Kim, Y. Kim, and S. Kim, "Learning loss for test-time augmentation," in *Advances in Neural Information Processing Systems (NeurIPS)*, 2020.
- [14] H. Talebi and P. Milanfar, "Learning to resize images for computer vision tasks," in *IEEE/CVF International Conference on Computer Vision (ICCV)*, 2021.
- [15] S. Enomoto, M. R. Busto, and T. Eda, "Dynamic test-time augmentation via differentiable functions," *arXiv preprint arXiv:2212.04681*, 2022.
- [16] J. Gao, J. Zhang, X. Liu, T. Darrell, E. Shelhamer, and D. Wang, "Back to the source: Diffusion-driven test-time adaptation," in *IEEE/CVF Conference on Computer Vision and Pattern Recognition (CVPR)*, 2023.
- [17] I. Gulrajani and D. Lopez-Paz, "In search of lost domain generalization," in *International Conference on Learning Representations (ICLR)*, 2020.
- [18] M. Zhang, S. Levine, and C. Finn, "Memo: Test time robustness via adaptation and augmentation," *Advances in Neural Information Processing Systems (NeurIPS)*, 2022.
- [19] P. T. Sivaprasad and F. Fleuret, "Test time adaptation through perturbation robustness," *arXiv preprint arXiv:2110.10232*, 2021.
- [20] D. Chen, D. Wang, T. Darrell, and S. Ebrahimi, "Contrastive test-time adaptation," in *IEEE/CVF Conference on Computer Vision and Pattern Recognition (CVPR)*, 2022.
- [21] D. Brahma and P. Rai, "A probabilistic framework for lifelong test-time adaptation," in *IEEE/CVF Conference on Computer Vision and Pattern Recognition (CVPR)*, 2023.
- [22] S. Goyal, M. Sun, A. Raghunathan, and J. Z. Kolter, "Test time adaptation via conjugate pseudo-labels," in *Advances in Neural Information Processing Systems (NeurIPS)*, 2022.
- [23] A. Bartler, A. Bühler, F. Wiewel, M. Döbler, and B. Yang, "Mt3: Meta test-time training for self-supervised test-time adaption," in *International Conference on Artificial Intelligence and Statistics (AISTATS)*, 2022.
- [24] A. Bartler, F. Bender, F. Wiewel, and B. Yang, "Ttaps: Test-time adaption by aligning prototypes using self-supervision," in *International Joint Conference on Neural Networks (IJCNN)*, 2022.
- [25] T. Kojima, Y. Matsuo, and Y. Iwasawa, "Robustifying vision transformer without retraining from scratch by test-time class-conditional feature alignment," in *International Joint Conference on Artificial Intelligence (IJCAI)*, 2022.
- [26] S. Jung, J. Lee, N. Kim, A. Shaban, B. Boots, and J. Choo, "Cafa: Class-aware feature alignment for test-time adaptation," in *IEEE/CVF International Conference on Computer Vision (ICCV)*, 2023.
- [27] K. Adachi, S. Yamaguchi, and A. Kumagai, "Covariance-aware feature alignment with pre-computed source statistics for test-time adaptation to multiple image corruptions," in *IEEE International Conference on Image Processing (ICIP)*, 2023.
- [28] Y. Iwasawa and Y. Matsuo, "Test-time classifier adjustment module for model-agnostic domain generalization," *Advances in Neural Information Processing Systems (NeurIPS)*, 2021.
- [29] J. S. Song, J. Lee, I.-S. Kweon, and S. Choi, "Ecotta: Memory-efficient continual test-time adaptation via self-distilled regularization," in *IEEE/CVF Conference on Computer Vision and Pattern Recognition (CVPR)*, 2023.
- [30] J. Kim, I. Hwang, and Y. M. Kim, "Ev-tta: Test-time adaptation for event-based object recognition," in *IEEE/CVF Conference on Computer Vision and Pattern Recognition (CVPR)*, 2022.
- [31] I. Shin, Y.-H. Tsai, B. Zhuang, S. Schuster, B. Liu, S. Garg, I. S. Kweon, and K.-J. Yoon, "Mm-tta: Multi-modal test-time adaptation for 3d semantic segmentation," in *IEEE/CVF Conference on Computer Vision and Pattern Recognition (CVPR)*, 2022.
- [32] A. Gunawan, M. A. Nugroho, and S. J. Park, "Test-time adaptation for real image denoising via meta-transfer learning," *arXiv preprint arXiv:2207.02066*, 2022.
- [33] S. Ebrahimi, S. O. Arik, and T. Pfister, "Test-time adaptation for visual document understanding," *arXiv preprint arXiv:2206.07240*, 2022.
- [34] F. Azimi, S. Palacio, F. Raue, J. Hees, L. Bertinetto, and A. Dengel, "Self-supervised test-time adaptation on video data," in *IEEE/CVF Winter Conference on Applications of Computer Vision (WACV)*, 2022.
- [35] S. Sinha, P. Gehler, F. Locatello, and B. Schiele, "Test: Test-time self-training under distribution shift," in *IEEE/CVF Winter Conference on Applications of Computer Vision (WACV)*, 2023.
- [36] Y. Zhang, S. Borse, H. Cai, and F. Porikli, "Auxadapt: Stable and efficient test-time adaptation for temporally consistent video semantic segmentation," in *IEEE/CVF Winter Conference on Applications of Computer Vision (WACV)*, 2022.
- [37] N. Chattopadhyay, S. Gehlot, and N. Singhal, "Fusion: Fully unsupervised test-time stain adaptation via fused normalization statistics," in *Computer Vision—ECCV 2022 Workshops: Tel Aviv, Israel, October 23–27, 2022, Proceedings, Part VII*, 2023.
- [38] V. Sharma, A. Diba, D. Neven, M. S. Brown, L. V. Gool, and R. Stiefelhagen, "Classification-driven dynamic image enhancement," in *IEEE/CVF Conference on Computer Vision and Pattern Recognition (CVPR)*, 2018.
- [39] H. Bahng, A. Jahanian, S. Sankaranarayanan, and P. Isola, "Exploring visual prompts for adapting large-scale models," *arXiv preprint arXiv:2203.17274*, 2022.
- [40] M. Jia, L. Tang, B.-C. Chen, C. Cardie, S. Belongie, B. Hariharan, and S.-N. Lim, "Visual prompt tuning," in *European Conference on Computer Vision (ECCV)*, 2022.
- [41] Y. Gao, X. Shi, Y. Zhu, H. Wang, Z. Tang, X. Zhou, M. Li, and D. N. Metaxas, "Visual prompt tuning for test-time domain adaptation," *arXiv preprint arXiv:2210.04831*, 2022.
- [42] Y. Gan, X. Ma, Y. Lou, Y. Bai, R. Zhang, N. Shi, and L. Luo, "Decorate the newcomers: Visual domain prompt for continual test time adaptation," in *Proceedings of the AAAI Conference on Artificial Intelligence (AAAI)*, 2023.
- [43] Y.-Y. Tsai, C. Mao, and J. Yang, "Convolutional visual prompt for robust visual perception," *Advances in Neural Information Processing Systems (NeurIPS)*, 2024.
- [44] S. Xie, R. Girshick, P. Dollár, Z. Tu, and K. He, "Aggregated residual transformations for deep neural networks," in *IEEE/CVF Conference on Computer Vision and Pattern Recognition (CVPR)*, 2017.
- [45] O. Ronneberger, P. Fischer, and T. Brox, "U-net: Convolutional networks for biomedical image segmentation," in *The Medical Image Computing and Computer Assisted Intervention Society (MICCAI)*, 2015.
- [46] J. Mei, Y. Han, Y. Bai, Y. Zhang, Y. Li, X. Li, A. Yuille, and C. Xie, "Fast advprop," in *International Conference on Learning Representations (ICLR)*, 2022.
- [47] S. Schneider, E. Rusak, L. Eck, O. Bringmann, W. Brendel, and M. Bethge, "Improving robustness against common corruptions by covariate shift adaptation," *Advances in Neural Information Processing Systems (NeurIPS)*, 2020.
- [48] H. Touvron, M. Cord, M. Douze, F. Massa, A. Sablayrolles, and H. Jegou, "Training data-efficient image transformers & distillation through attention," in *International Conference on Machine Learning (ICML)*, 2021.
- [49] D. Hendrycks, N. Mu, E. D. Cubuk, B. Zoph, J. Gilmer, and B. Lakshminarayanan, "AugMix: A simple data processing method to improve robustness and uncertainty," in *International Conference on Learning Representations (ICLR)*, 2020.
- [50] D. Hendrycks, S. Basart, N. Mu, S. Kadavath, F. Wang, E. Dorundo, R. Desai, T. Zhu, S. Parajuli, M. Guo *et al.*, "The many faces of robustness: A critical analysis of out-of-distribution generalization," in *IEEE/CVF International Conference on Computer Vision (ICCV)*, 2021.
- [51] A. Dosovitskiy, L. Beyer, A. Kolesnikov, D. Weissenborn, X. Zhai, T. Unterthiner, M. Dehghani, M. Minderer, G. Heigold, S. Gelly *et al.*, "An image is worth 16x16 words: Transformers for image recognition at scale," in *International Conference on Learning Representations (ICLR)*, 2020.

Supplementary Materials for Test-time Adaptation Meets Image Enhancement: Improving Accuracy via Uncertainty-aware Logit Switching

arXiv:2403.17423v1 [cs.CV] 26 Mar 2024

TABLE VII
AVERAGE CLASSIFICATION ERROR RATE OF RESNET-50 FOR THE DIVERSE IMAGE NET CTTA TASK.

TECA	Source	Input Adapt	BN Adapt	Tent	EATA	CoTTA
	82.35	76.60	72.07	66.52	66.61	63.20
✓			69.60	65.13	64.20	61.29

TABLE VIII
AVERAGE CLASSIFICATION ERROR RATE OF RESNET-50 FOR THE GRADUAL IMAGE NET CTTA TASK.

TECA	Source	Input Adapt	BN Adapt	Tent	EATA	CoTTA
	59.61	54.86	51.41	52.09	46.70	40.66
✓			49.73	57.20	45.38	39.23

Abstract—The supplementary materials for “Test-time Adaptation Meets Image Enhancement: Improving Accuracy via Uncertainty-aware Logit Switching.” The additional experimental results are provided.

VI. CTTA DIVERSE AND GRADUAL TASKS

In the diverse task, we evaluated the average of 10 trials in different evaluation orders of the corrupted test set. In the gradual task, the evaluation order of the corrupted test set is the same as in the standard task, and the corruption severity level is varied in steps of 1→2→3→4→5→4→3→2→1.

Table VII shows the results of the diverse task. As with the standard task, TECA consistently improves the average error rate of the TTA methods. Due to the irregularity of the corruption order in the diverse task, CoTTA, which is robust against large distribution shifts, performs well. Furthermore, the combination of CoTTA and TECA reduces the average error rate by 2.01 points over CoTTA alone.

Table VIII shows the results of the gradual task. With the exception of Tent, TECA improves the average error rate of the TTA methods. Tent shows a higher error rate than BN Adapt, which indicates that training the BN parameters by Tent is detrimental in long-term adaptation tasks. The error rate of TECA is higher than that of the original Tent because TECA increases the number of BN parameters to be trained and the impact of error accumulation is greater. As with the diverse tasks, CoTTA performs better than the other TTA methods, with the best results obtained by combining it with TECA.

From these CTTA task results, we found that a combination of TECA and TTA methods improves performance more in various situations.

VII. RESULTS OF THE PTTA TASK

In the PTTA task, we used Dirichlet distributions to generate streaming data that are correlated between test samples and simulated real-world applications. For the PTTA task, we use *RoTTA* [1], a TTA method that allows stable adaptation by using a memory bank under correlated non-i.i.d. data streams.

We show the results of the PTTA task in Table IX. TECA increases the accuracy even for *RoTTA*, the state-of-the-art method in realistic tasks. Combining *RoTTA* with TECA shows the best results, reducing the error rate by 0.99 points over *RoTTA* alone. For late-time corruptions (pixelate and jpeg), TECA increases the *RoTTA* error rate. Incorporating a method such as CoTTA, which is more robust against long-term, drastically changing distribution shifts, may solve this problem.

VIII. DETAILED RESULTS OF THE DOMAIN GENERALIZATION BENCHMARKS

Tables X–XIII show the results for each domain generalization dataset.

IX. COMPUTATIONAL TIME

TECA requires more computation time than the original TTA method because it performs inference of the image enhancement model and of the classification model for the enhanced images. We measured the computation time and error rate for the original TTA methods and their combination with TECA, which are shown in Figure 5. We experimented with a single NVIDIA-A100 GPU in the same setup as Figure 4 in main paper. Combining TECA decreases the error rate for all methods, but increases the computation time. However, the combination of Tent and TECA improves the tradeoff between error rate and computation time over CoTTA, the state-of-the-art TTA method.

X. EFFECTS OF THE IMAGE ENHANCEMENT MODEL AND LS ON CONFIDENCE SCORES

We show a histogram of confidence scores in Figure 6 to demonstrate the effects of the image enhancement model and LS. The image enhancement model reduces the number of confidence scores around 0, and LS further reduces this.

TABLE IX
CLASSIFICATION ERROR RATE OF RESNET-50 FOR THE IMAGENET PTTA TASK.

Time	t																
Method	TECA	motion	snow	fog	shot	defocus	contrast	zoom	brightness	frost	elastic	glass	Gaussian	Pixelate	jpeg	impulse	Mean ↓
Source		86.82	84.37	77.25	94.56	84.83	95.57	77.15	44.34	79.74	85.21	91.09	95.30	76.91	66.65	95.30	82.34
Input Adapt		85.05	80.32	70.89	82.56	84.13	89.31	77.77	44.84	74.76	81.02	90.33	83.05	<u>62.16</u>	59.43	83.01	76.57
RoTTA		79.53	<u>72.27</u>	<u>57.30</u>	88.80	87.74	81.88	<u>66.77</u>	37.88	<u>67.88</u>	59.75	83.85	88.60	60.77	65.15	88.92	72.47
RoTTA	✓	75.92	68.02	55.06	<u>83.25</u>	85.85	77.67	64.71	37.80	66.19	59.57	<u>84.01</u>	<u>84.99</u>	64.97	75.70	<u>88.50</u>	71.48

TABLE X
CLASSIFICATION ACCURACY OF RESNET-50 ON THE VLCS DATASET.

Method	TECA	C	L	S	V	Mean ↑
Source		97.3 ± 0.3	64.0 ± 0.6	71.1 ± 0.8	73.2 ± 0.5	76.4
Input Adapt		97.4 ± 0.7	63.8 ± 0.2	69.0 ± 1.0	73.0 ± 0.7	75.8
T3A		98.6 ± 0.1	64.7 ± 0.5	71.4 ± 1.0	72.7 ± 0.7	76.8
T3A	✓	98.2 ± 0.3	63.8 ± 0.4	71.7 ± 1.7	72.8 ± 0.9	76.6

TABLE XI
CLASSIFICATION ACCURACY OF RESNET-50 ON THE PACS DATASET.

Method	TECA	A	C	P	S	Mean ↑
Source		82.2 ± 0.6	80.7 ± 1.5	96.6 ± 0.5	78.4 ± 1.4	84.5
Input Adapt		84.0 ± 0.3	80.1 ± 1.2	96.4 ± 0.3	80.5 ± 1.1	85.2
T3A		83.2 ± 0.6	82.0 ± 1.2	96.9 ± 0.3	79.5 ± 1.4	85.4
T3A	✓	84.8 ± 0.4	81.9 ± 1.0	96.9 ± 0.4	80.8 ± 1.3	86.1

TABLE XII
CLASSIFICATION ACCURACY OF RESNET-50 ON THE OFFICEHOME DATASET.

Method	TECA	A	C	P	R	Mean ↑
Source		60.6 ± 0.8	54.2 ± 0.4	75.5 ± 0.4	76.9 ± 0.3	66.8
Input Adapt		60.6 ± 0.5	54.6 ± 0.2	75.2 ± 0.4	76.6 ± 0.1	66.8
T3A		60.9 ± 0.4	55.8 ± 0.5	77.1 ± 0.6	77.6 ± 0.3	67.8
T3A	✓	61.4 ± 0.4	56.0 ± 0.4	77.1 ± 0.5	77.3 ± 0.2	67.9

TABLE XIII
CLASSIFICATION ACCURACY OF RESNET-50 ON THE TERRAINCOGNITA DATASET.

Method	TECA	L100	L38	L43	L46	Mean ↑
Source		46.4 ± 2.4	44.6 ± 1.8	51.1 ± 0.9	40.0 ± 0.8	45.5
Input Adapt		48.2 ± 2.1	43.6 ± 1.2	52.4 ± 0.1	38.6 ± 1.3	45.7
T3A		43.2 ± 2.0	46.0 ± 0.8	46.6 ± 1.0	38.2 ± 0.5	43.5
T3A	✓	47.6 ± 1.7	45.5 ± 1.4	47.6 ± 1.0	37.6 ± 1.0	44.6

The image enhancement model and LS contribute to obtaining pseudo-labels that are closer to hard labels by increasing the number of confidence scores around 1.0.

XI. VISUALIZATION OF ENHANCED IMAGES

This section provides the same as the visualization in Figure 3, we show the original and enhanced images and their confidence scores for each corruption in the ImageNet-C dataset. Figure 7–21 show the results.

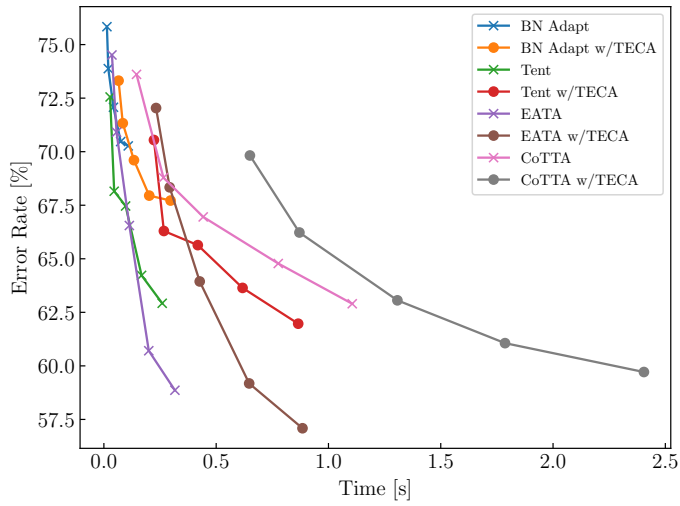


Fig. 5. Trade-off between error rate and computation time for the standard ImageNet CTTA task. We compared the TTA method with TECA using ResNet-18, 34, 50, 101, and 152 as classification models.

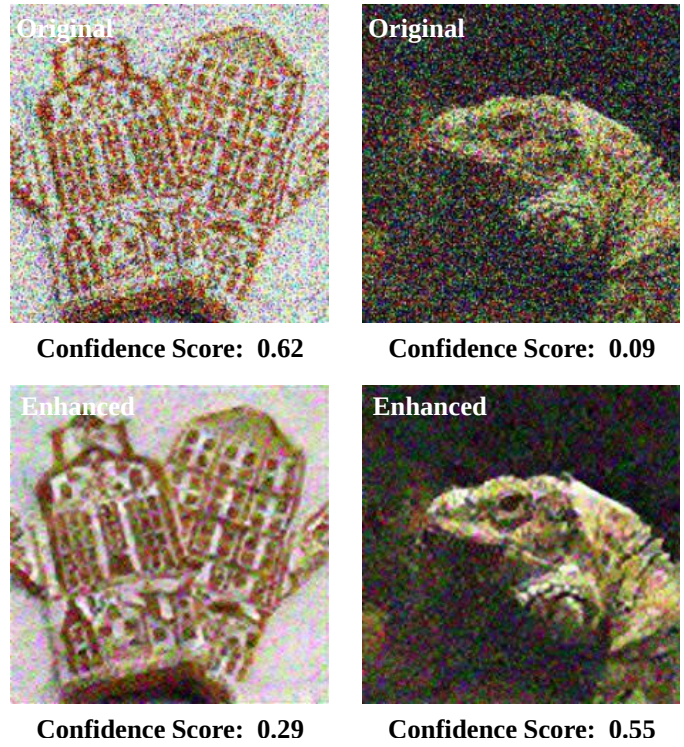


Fig. 7. Gaussian noise at severity level 5 images and URIE enhanced images and their confidence scores in the ImageNet-C dataset. The top and bottom rows are the original and enhanced images, respectively.

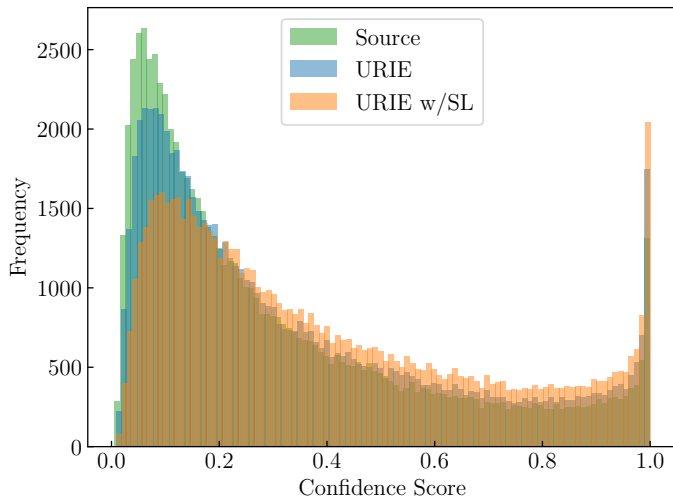


Fig. 6. Confidence score histograms for each approach: Source, Input Adapt by URIE, and Input Adapt by URIE combined with LS. We used the ResNet-50 classification model with in the standard ImageNet CTTA task.

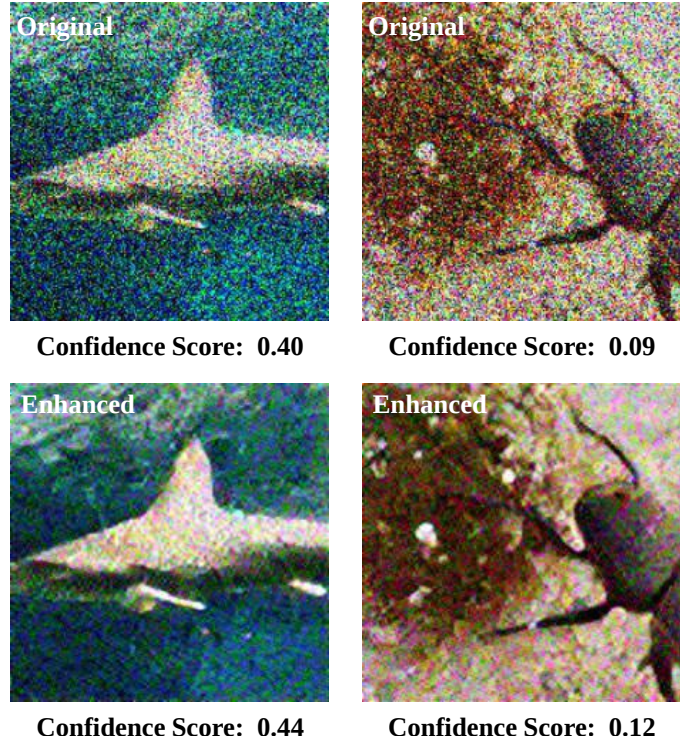
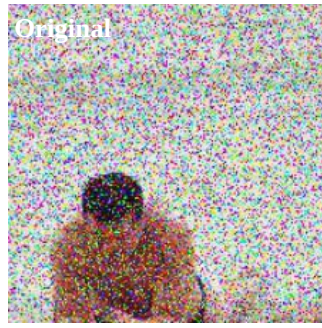


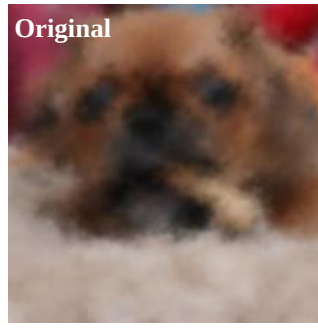
Fig. 8. Shot noise at severity level 5 images and URIE enhanced images and their confidence scores in the ImageNet-C dataset. The top and bottom rows are the original and enhanced images, respectively.



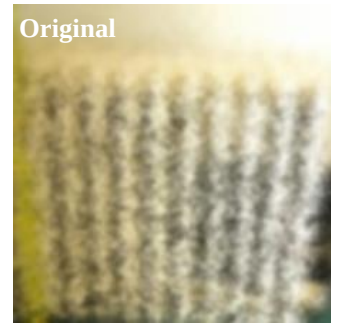
Confidence Score: 0.31



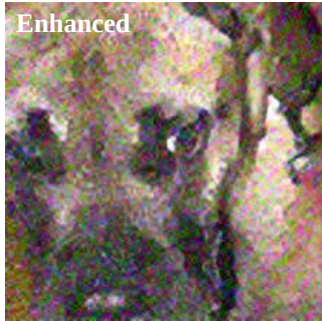
Confidence Score: 0.23



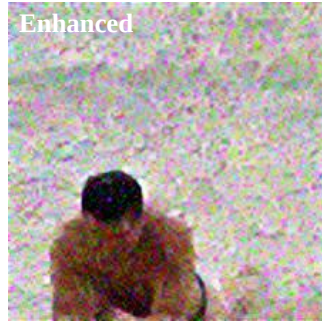
Confidence Score: 0.27



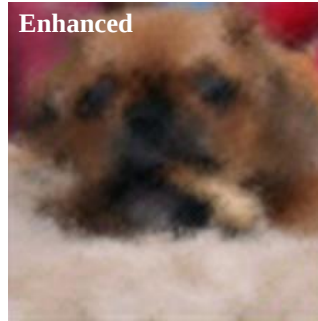
Confidence Score: 0.17



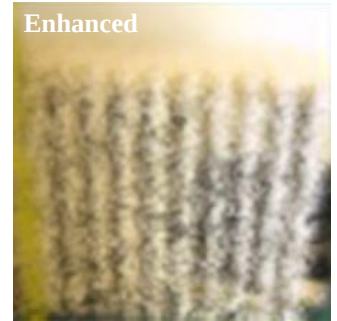
Confidence Score: 0.35



Confidence Score: 0.05



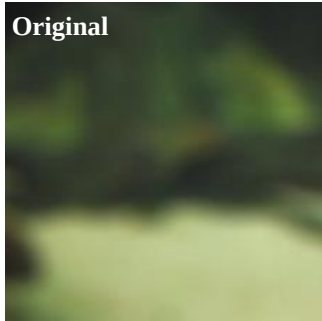
Confidence Score: 0.17



Confidence Score: 0.15

Fig. 9. Impulse noise at severity level 5 images and URIE enhanced images and their confidence scores in the ImageNet-C dataset. The top and bottom rows are the original and enhanced images, respectively.

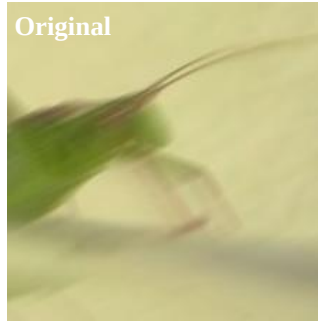
Fig. 11. Glass blur at severity level 5 images and URIE enhanced images and their confidence scores in the ImageNet-C dataset. The top and bottom rows are the original and enhanced images, respectively.



Confidence Score: 0.02



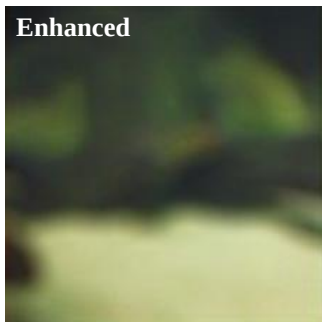
Confidence Score: 0.05



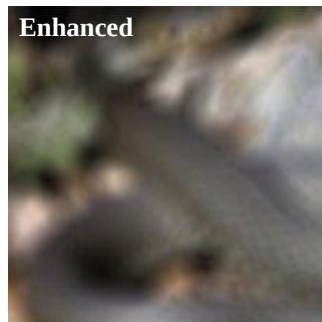
Confidence Score: 0.43



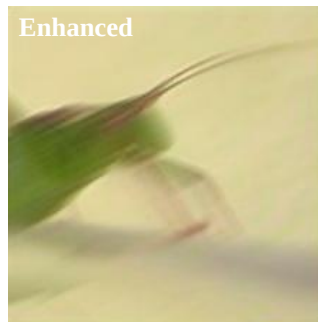
Confidence Score: 0.28



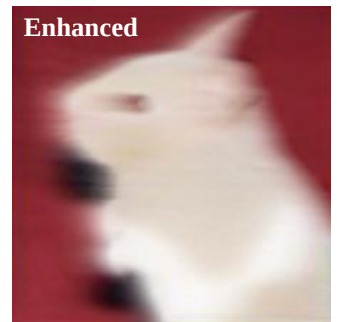
Confidence Score: 0.02



Confidence Score: 0.07



Confidence Score: 0.37



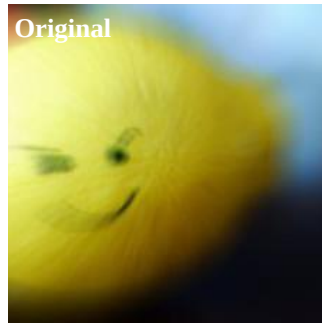
Confidence Score: 0.30

Fig. 10. Defocus blur at severity level 5 images and URIE enhanced images and their confidence scores in the ImageNet-C dataset. The top and bottom rows are the original and enhanced images, respectively.

Fig. 12. Motion blur at severity level 5 images and URIE enhanced images and their confidence scores in the ImageNet-C dataset. The top and bottom rows are the original and enhanced images, respectively.



Confidence Score: 0.17



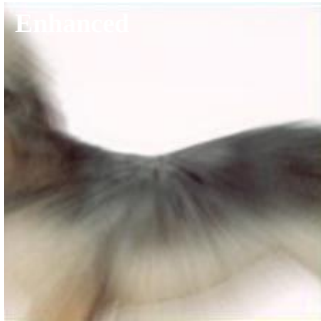
Confidence Score: 0.28



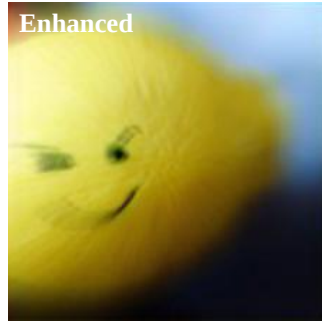
Confidence Score: 0.67



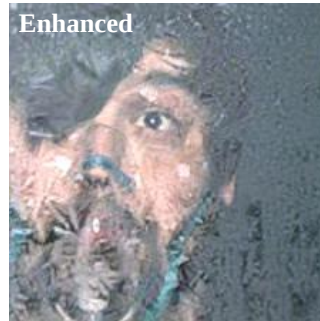
Confidence Score: 0.53



Confidence Score: 0.20



Confidence Score: 0.30



Confidence Score: 0.16



Confidence Score: 0.22

Fig. 13. Zoom blur at severity level 5 images and URIE enhanced images and their confidence scores in the ImageNet-C dataset. The top and bottom rows are the original and enhanced images, respectively.

Fig. 15. Frost at severity level 5 images and URIE enhanced images and their confidence scores in the ImageNet-C dataset. The top and bottom rows are the original and enhanced images, respectively.



Confidence Score: 0.92



Confidence Score: 0.31



Confidence Score: 0.15



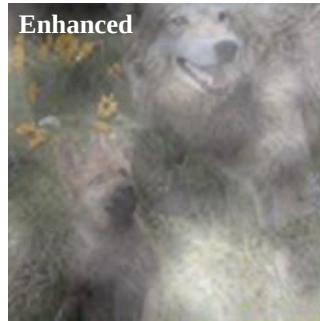
Confidence Score: 0.67



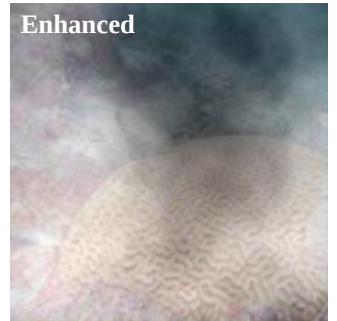
Confidence Score: 0.41



Confidence Score: 0.35



Confidence Score: 0.24



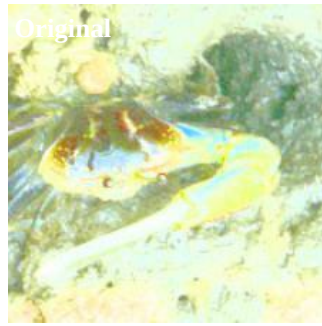
Confidence Score: 0.97

Fig. 14. Snow at severity level 5 images and URIE enhanced images and their confidence scores in the ImageNet-C dataset. The top and bottom rows are the original and enhanced images, respectively.

Fig. 16. Fog at severity level 5 images and URIE enhanced images and their confidence scores in the ImageNet-C dataset. The top and bottom rows are the original and enhanced images, respectively.



Confidence Score: 0.31



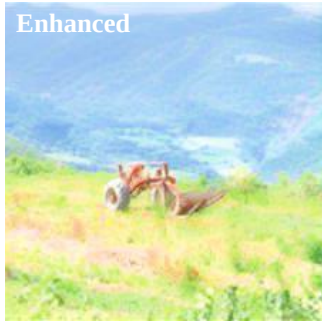
Confidence Score: 0.17



Confidence Score: 0.36



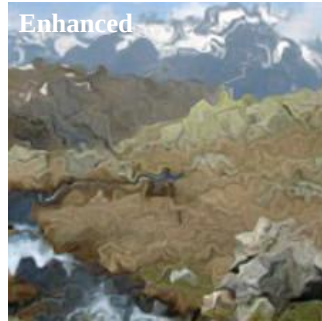
Confidence Score: 0.42



Confidence Score: 0.55



Confidence Score: 0.64



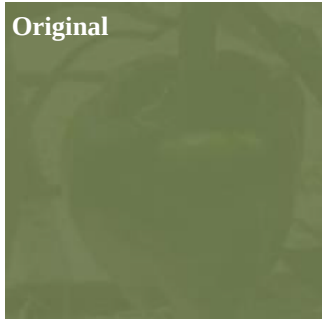
Confidence Score: 0.26



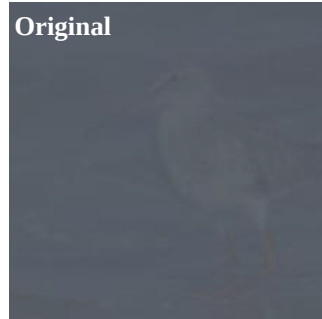
Confidence Score: 0.31

Fig. 17. Brightness at severity level 5 images and URIE enhanced images and their confidence scores in the ImageNet-C dataset. The top and bottom rows are the original and enhanced images, respectively.

Fig. 19. Elastic transform at severity level 5 images and URIE enhanced images and their confidence scores in the ImageNet-C dataset. The top and bottom rows are the original and enhanced images, respectively.



Confidence Score: 0.25



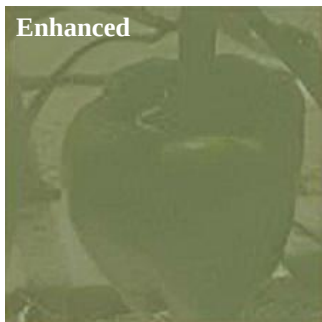
Confidence Score: 0.21



Confidence Score: 0.60



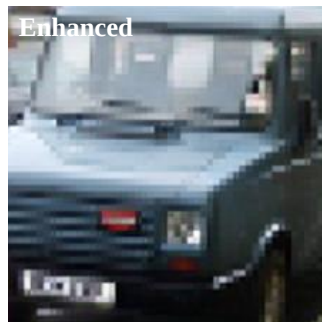
Confidence Score: 0.28



Confidence Score: 0.46



Confidence Score: 0.86



Confidence Score: 0.27



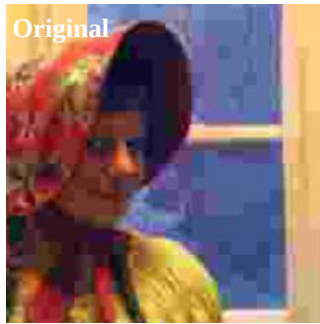
Confidence Score: 0.46

Fig. 18. Contrast at severity level 5 images and URIE enhanced images and their confidence scores in the ImageNet-C dataset. The top and bottom rows are the original and enhanced images, respectively.

Fig. 20. Pixelate at severity level 5 images and URIE enhanced images and their confidence scores in the ImageNet-C dataset. The top and bottom rows are the original and enhanced images, respectively.



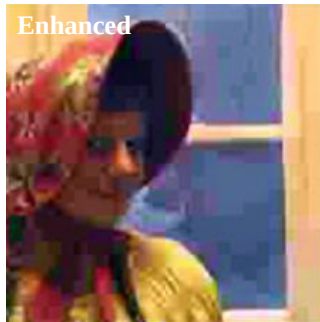
Confidence Score: 0.65



Confidence Score: 0.16



Confidence Score: 0.49



Confidence Score: 0.15

Fig. 21. Jpeg compression at severity level 5 images and URIE enhanced images and their confidence scores in the ImageNet-C dataset. The top and bottom rows are the original and enhanced images, respectively.

REFERENCES

- [1] L. Yuan, B. Xie, and S. Li, "Robust test-time adaptation in dynamic scenarios," in *IEEE/CVF Conference on Computer Vision and Pattern Recognition (CVPR)*, 2023.